Numerical evaluation of plastic rotation capacity in RC beams

A.L. Gamino & T.N. Bittencourt
Structural and Geotechnical Engineering Department, Polytechnical School of São Paulo University, São Paulo, Brazil

ABSTRACT: The objective of the present paper is the analysis of the parameter "θ_{pl}" in reinforced-concrete beams by means of smeared crack approaches. The effects of the compressive strength and the size dependence in bending are re-investigated. The non-linear analyses were carried out by means of the Finite Element Method. The programs DIANA, CASTEM2000, and QUEBRA2D/FEMOOP were used in the numerical simulations. Appropriate constitutive models for concrete, rebars and bond-slip interfaces were implemented to represent more realistically the behavior of the structural system. Interface and reinforcement (discrete and embedded approaches) finite elements were used to accomplish an explicit representation of the concrete-reinforcement bond.

1 INTRODUCTION

Since the publication of Kani in 1967, it is known that the resistant capacity of beams is highly dependent on size effects. In 1966 Corley (1966) advocated that size effect did not significantly affect the plastic rotation capacity "θpl" in R/C beams.

However, in 1988 Hillerborg (1988) concluded, using fracture mechanics concepts, that "θpl" in R/C sections is inversely proportional to the height of the structural element.

Over the last decades research on ductility of beams has evolved and demonstrated the influence of the reinforcement ratio, concrete grade, stirrup spacing and finally size effects.

The importance of the size effect in beams of reinforced-concrete is in fact that this can cause reductions in the capacities of inelastic deformation and plastic rotation as well as transition of types of brittle/ductile ruptures.

These effects can appear in two forms:

Modifications in the "a/d" relations ("a" is the shear span; "d" is the effective beam depth) that over all affect the load capacity of the beams to the shear Walraven & Lehwalter (1994);

Variations in the slenderness inside or out of pure bending regions;

The first research on ductility of beams had involved to portray the influence of the reinforced ratio Leslie, Rajagopalan & Everard (1976), strength of the concrete Tognon et al. (1980), Ashour (2000), span between stirrups Shin et al. (1989) and finally size effect Alca et al. (1997).

This work is concentrated on the evaluation of the ductility in 2D beams using smeared crack models in the concrete. The numerical 2D analysis is based on the finite element method implemented in CASTEM 2000 developed by the Département de Mécanique et de Technologie (DMT) du Commissariat Français à l´Energie Atomique (CEA). This program uses the constitutive elastoplastic perfect model for the steel, the Drucker-Prager two parameter model for the concrete and the Newton-Raphson for the solution of non-linear systems.

In the QUEBRA2D/FEMOOP system appropriate constitutive models for concrete, rebars and bond-slip interfaces have been implemented to represent more realistically the behavior of the structural system. Interface and reinforcement (discrete and embedded approaches) finite elements have been used to accomplish an explicit representation of the concrete-reinforcement bond.

In the numerical 2D simulations, the established computational program in the Finite Element Method DIANA was developed by the TNO Building and Constructions Research of the Department of Computational Mechanics (Netherlands). First, the influence of each smeared crack model on the numerical results was presented. Later, a parametric study is carried out. An analytical model is presented in order to calculate the plastic rotation capacity "θpl" of the analyzed beams. Later the experimental results are compared with the results from the numerical simulations.

2 NUMERICAL EVALUATION OF PLASTIC ROTATION CAPACITY

2.1 *Concrete Constitutive Model in CASTEM 2000*

The concrete constitutive model used was the Drucker-Prager two parameters model (derived from the Ottosen four parameters model). This model was formulated in 1952 and can be seen as a simple modification of the criterion of Von Mises, including the influence of the hydrostatic pressure, according to Equation (1).

$$f(\sigma) = \alpha I_1 + \sqrt{J_2} - k_{dp} = 0 \quad (1)$$

where "α" and "kdp" are the material constants, "I1" and "J2" the invariants that depend on the normal stress on a body. Figure 1 brings the graphical representation of the surface of plasticity in the plan σ1-σ2 where "ft" is the tensile strength, "fc" is the compressive strength and "fbc" is the biaxial strength in compression.

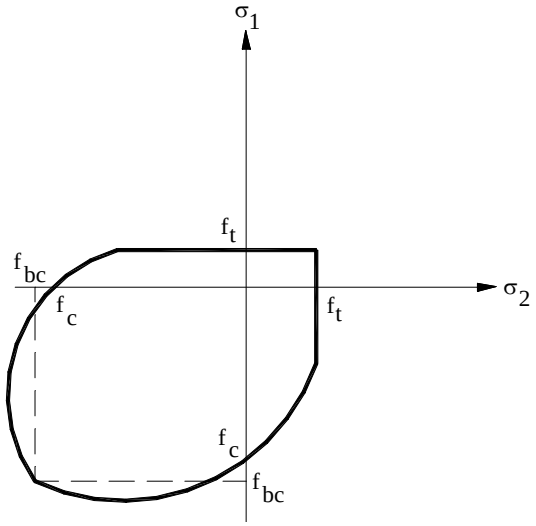

Figure 1. Drucker-Prager yield criteria.

2.2 *Concrete Constitutive Models in DIANA*

2.2.1 *Hardening Effect*

For the concrete under compression the model described in the code (CEB-Fip, 1993) was used in some modeling represented in the Equation 2.

$$\frac{\sigma_c}{f_{cm}} = \frac{\frac{E_{ci}}{E_{c1}}\frac{\varepsilon_c}{-0{,}22\%} - \left(\frac{\varepsilon_c}{-0{,}22\%}\right)^2}{1 + \left(\frac{E_{ci}}{E_{c1}} - 2\right)\frac{\varepsilon_c}{-0{,}22\%}} \quad (2)$$

In other modeling the non-linear hardening model of *Thorenfeldt* was used. This model presented in Figure 2 uses an equation between compressive stress and the deformations based in the adoption of diverse parameters.

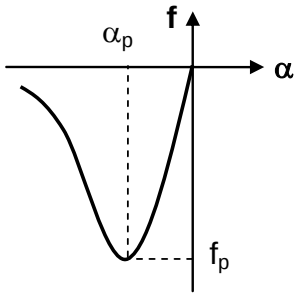

Figure 2. *Thorenfeldt* hardening curve.

2.2.2 *Softening Effect*

For the corresponding curve to the behavior of the concrete under traction the described bilinear model for the code (CEB-Fip, 1993) was used in some analyses in agreement with to Equation 3.

$$\bar{\sigma} = -\frac{(f_{ctm} - 2{,}12)}{\left(0{,}015 - \bar{\varepsilon}\right)}.0{,}015 + f_{ctm} \quad (3)$$

In other simulations the non-linear curve of Hordijk was used. This model presented in Figure 3 uses an exponential relation between the normal tensile stress and the deformations, with "c1" and "c2" assuming the values respectively of 3,0 and 6,93.

$$\frac{\sigma^{cr}(\varepsilon^{cr})}{f_t} = \begin{cases} \left(1 + \left(c_1 \frac{\varepsilon^{cr}}{\varepsilon_{ult}}\right)^3\right) exp\left(-c_2 \frac{\varepsilon^{cr}}{\varepsilon_{ult}}\right) \ldots \\ -\frac{\varepsilon^{cr}}{\varepsilon_{ult}}\left(1 + c_1^3\right) exp(-c_2), for \rightarrow 0 < \varepsilon^{cr} < \varepsilon_{ult} \\ 0, for \rightarrow \varepsilon_{ult} < \varepsilon^{cr} < \infty \end{cases}$$

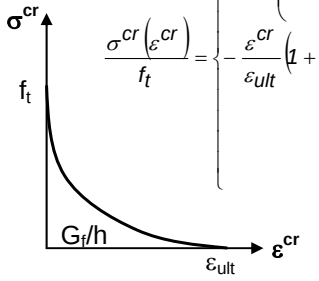

Figure 3. Hordijk softening curve.

Three smeared crack models were available in this program: fixed, multi-directional and rotating.

2.3 *Concrete Constitutive Model in FEMOOP*

A four parameter model of Ottosen (1977) was used to represent an uncracked material structure. The rupture surface is given by:

$$F = A\frac{J_2}{f_{cm}^2} + \lambda\frac{\sqrt{J_2}}{f_{cm}} + B\frac{I_1}{f_{cm}} - 1 = 0 \quad (4)$$

A linear softening curve law was utilized to represent the cracked region with a rotating smeared-crack model.

The contact and truss finite elements were implemented (discrete and embedded approach in agreement with Elwi & Hrudey (1989) formulations) for the numerical representation of rebars and interfaces.

2.4 *Steel Reinforcements*

In all programs the reinforcements were modeled with the Von Mises plasticity model.

2.5 *Steel Bonding Model in FEMOOP*

The Homayoun & Mitchell (1996) multilinear bond-slip model described in Figure 4 was implemented for the representation of interfaces (concrete/steel) behavior. The following parameters are given: τ_{sf} is the interface bond strength, τ_{sr} is the interface residual bond strength, s_f is the interface slip at the peak stress, s_r is the residual interface slip, E_b is the pre-peak bond modulus and E_d is the post-peak bond modulus.

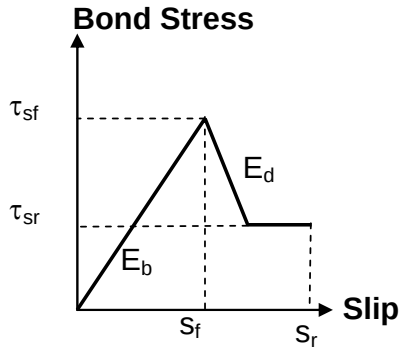

Figure 4. *Homayoun* bond-slip curve.

3 THEORETICAL ANALYSIS OF PLASTIC ROTATING CAPACITY

Using the MC-90 the plastic rotation capacity can be defined as:

$$\theta_{pl} = \int_{a=0}^{l_{pl}} \frac{1}{d - x(a)} \left[\varepsilon_{sm}(a) - \varepsilon_{smy}\right] da \qquad (5)$$

where $\varepsilon_{sm}(a)$ is the reinforced strain in the member plastification place, ε_{smy} is the reinforced deformation for crack tension equal to f_{yk}.

Using the definition and applying the model $\sigma s(\varepsilon sm)$ by Kreller (1989):

$$\theta_{pl} = \int_{a=0}^{l_{pl}} \frac{0{,}8}{d - x} \left(1 - \frac{\sigma_{sr1}}{f_{yk}}\right) \left(\varepsilon_{s2} - \varepsilon_{sy}\right) dx \qquad (6)$$

where σ_{sr1} is the reinforced stress in the crack, ε_{s2} and ε_{sy} respectively are the yield deformations in steel reinforcements and cracks.

The Figure 5 represents the process of the plastic rotating capacity using an equivalent beam.

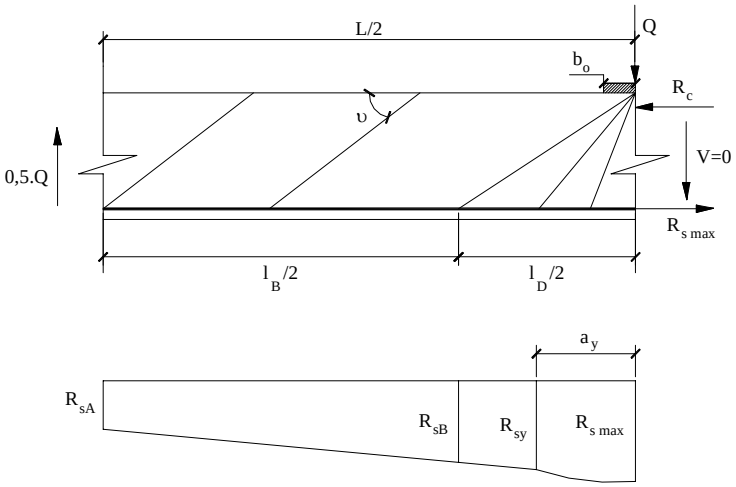

Figure 5. Equivalent beam.

By using the Figure 5 can be calculated the concrete and steel forces:

$$\begin{aligned} R_c &= -M / z + N.z_s / z + 0{,}5.V.\cot\upsilon \\ R_s &= M / z + N.(1 - z_s / z) + 0{,}5.V.\cot\upsilon \end{aligned} \qquad (7)$$

where υ is the inclination angle of the compression field.

The tensile forces can be derived from the following form:

$$R_s(x) = R_{s,max} - 4.(R_{s,max} - R_{sB}).(x / l_D)^2 \rightarrow x \le l_D / 2$$

$$R_s(x) = R_{sA} + \frac{R_{sB} - R_{sA}}{l_B}.(L - 2x) \rightarrow L / 2 \ge x \ge l_D / 2 \qquad (8)$$

And from this form is found the length of the plasticized zone:

$$a_y = \frac{l_{pl}}{2} = 0{,}5.l_D.\sqrt{\frac{R_{s\,max} - R_{sy}}{R_{s\,max} - R_B}} \rightarrow R_{sy} > R_{sB} \qquad (9)$$

$$a_y = \frac{l_{pl}}{2} = 0{,}5.\left(L - l_B \frac{R_{sy} - R_{sA}}{R_B - R_{sA}}\right) \rightarrow R_{sy} \le R_{sB}$$

Solving the integral of Equation (6) the plastic rotation capacity can be calculated:

$$\theta_{pl} = \frac{2.\delta}{3(d - x)} \left(1 - \frac{\sigma_{sr1}}{f_{yk}}\right) \frac{l_D}{A_s E_s} \sqrt{\frac{(R_{s\,max} - R_{sy})^3}{R_{s\,max} - R_{sB}}}$$

$$R_{sy} \geq R_{sB} \tag{10}$$

$$\theta_{pl} = \frac{2.\delta}{d-x}\left(1-\frac{\sigma_{sr1}}{f_{yk}}\right)\frac{l_D}{A_S E_S}\left[\frac{l_D}{3}\left(2.R_{s\,max}-3.R_{sy}+R_{sB}\right)+\frac{l_B}{2}\frac{\left(R_{sB}-R_{sy}\right)^2}{\left(R_{sB}-R_A\right)}\right]$$

$$R_{sy} \leq R_{sB}$$

Making the width of the support plate (b_o=0) and leaving the effect of the shear forces (cot υ=0) arrived the following expressions are found:

$$a_y = \frac{l_{pl}}{2} = \frac{L}{2}\left(1-\frac{M_y}{M_u}\right) \tag{11}$$

$$\theta_{pl} = a_y.\frac{M_u - M_y}{(EI)_{pl}} = \frac{L}{2.(EI)_{pl}}\frac{(M_u - M_y)^2}{M_u}$$

4 ANALYSIS OF THE SMEARED CRACK APPROACH

Three reinforced-concrete beams were analyzed in the computational program DIANA, analyzed in the experimental program of Barbosa (1998) every 3,60m of span, width of 15cm and height of 28,3cm, with stirrups of 6mm a diameter spaced in 8cm and with applied loads in 1/3 and 2/3 of span. The longitudinal bottom reinforcements consist of two bars of 16mm a diameter and the longitudinal top reinforcements consist of two bars of 8mm a diameter. The mechanical properties of these beams is shown in Table 1.

Table 1. Material properties.

Beam	f_c(MPa)	f_y(MPa)	E_c(GPa)	E_s(GPa)
01	40	620	38,2	210
02	75	830	42	210
03	100	830	51,2	210

In the modeling the three models of smeared cracks (fixed, rotating and multi-directional) without softening (brittle model) and hardening model in agreement to proposal of Thorenfeldt for two distinct values of the shear retention factor (β). In the fixed model (Figure 6) the use of a smaller shear retention factor implied in a more extended cracking; the variations in β had not modified the maximum values of the crack deformations (ε^{nncr}). In the multi-directional model (Figure 7) the use of a smaller shear retention factor implied in a more extended cracking mainly in the region of pure bending (for β=0,2 notices eight wider cracks in this region were noticed; for β=0,9 six wider cracks in the same region were noticed); the variations in "β" had modified the maximum values of the crack deformations ("β" is inversely proportional to "ε^{nncr}" in this model).

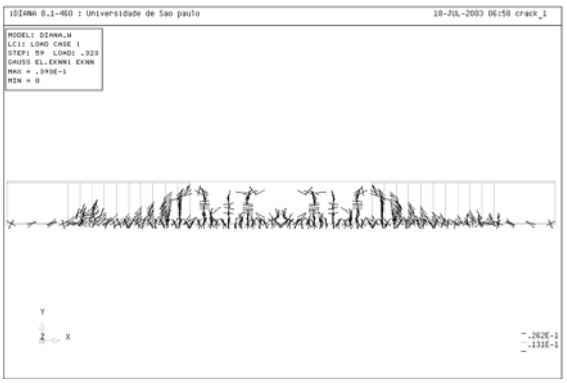

β=0,2

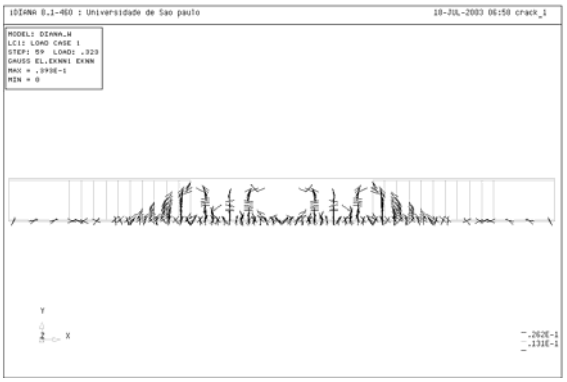

β=0,9

Figure 6. Crack pattern for fixed-crack approach.

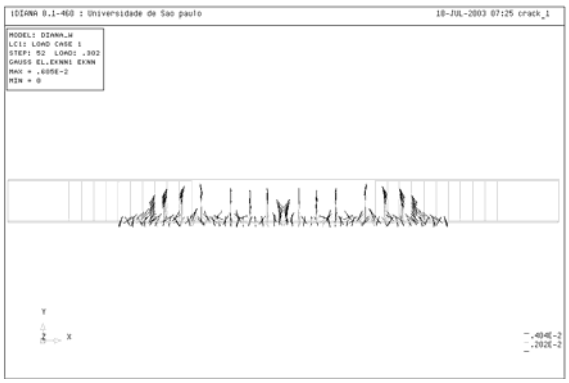

β=0,2

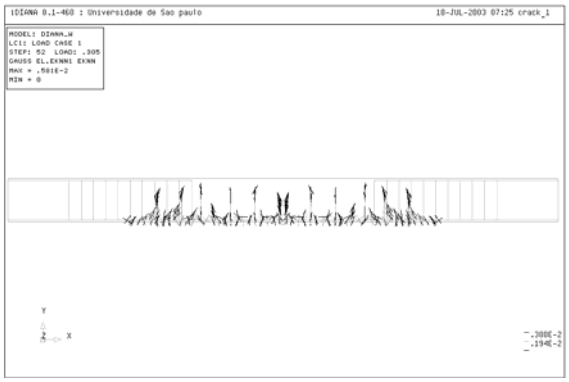

β=0,9

Figure 7. Crack pattern for multi-directional approach.

In the rotating model (Figure 8) the use of a smaller shear retention factor implied in a more extended cracking mainly is of the region of pure

bending; variations in "β" had very affected the values of the deformations in the cracks. The fixed, multi-directional and rotating models predicted respectively six, eight and four wider cracks (for β=0,2) in the region of pure bending. The experimental crack pattern (Figure 9) shows four wider cracks similar to the ones found with the rotating smeared crack model.

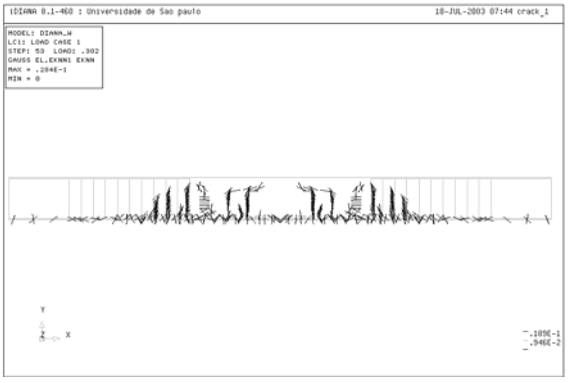

β=0,2

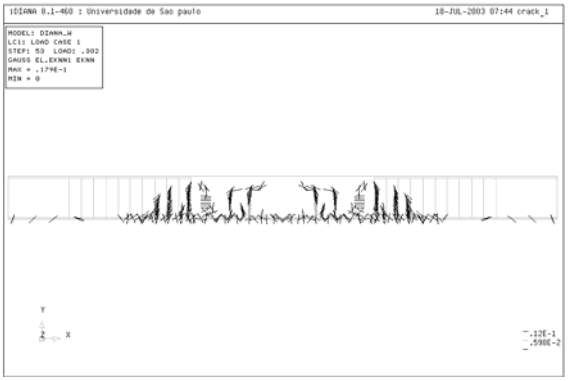

β=0,9

Figure 8. Crack pattern for rotating model.

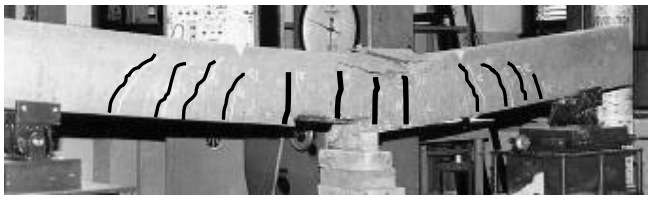

Figure 9. Experimental crack pattern.

5 ANALYSIS OF THE PLASTIC ROTATION CAPACITY

The plastic rotation capacity for the force-displacement curves was evaluated for experimental and numerical modeling in DIANA, CASTEM and QUEBRA2D/FEMOOP programs for the three previous beams.

Each "θpl" was calculated using the Equation (11). The calculated values were disposed in Table 2. In general, the results from the DIANA were a little more rigid than the experimental results and the results in platform CASTEM were a little less rigid than the experimental ones, whose influence can be observed in the values of found for the plastic rotation capacity: bigger values for the numerical simulation in the DIANA and smaller values for CASTEM. The results found with FEMOOP were located between the DIANA and the CASTEM results (closer to the experimental results).

Table 2. Plastic rotation capacity values.

	Beam	a_y(cm)	θ_{pl}(mrad)
Experiment	01	2,63	21,69
	02	13,17	25,86
	03	31,31	33,93
CASTEM	01	1,87	21,02
	02	7,48	28,32
	03	16,62	38,90
DIANA	01	4,32	22,93
	02	1,32	21,29
	03	6,14	28,30
FEMOOP	01	3,36	22,66
	02	9,66	24,29
	03	27,77	29,77

Table 3 illustrates the displacements at the steel yield stress (δy), displacements in the rupture (δu) and global ductility ratio (μ=δu/δy) from the experimental and numerical analysis.

Table 3. Ductility ratio values.

	Beam	δ_u(mm)	δ_y(mm)	$\mu_d = \delta_u/\delta_y$
Experiment	01	29,52	12,31	2,40
	02	73,53	21,87	3,36
	03	71,94	13,55	5,30
CASTEM	01	29,18	15,16	1,92
	02	70,15	22,89	3,06
	03	69,23	22,30	3,10
DIANA	01	20,5	13,30	1,54
	02	38	23,60	1,61
	03	45,7	21,9	2,09
FEMOOP	01	26,8	14,6	1,83
	02	44,2	22,6	1,96
	03	49,3	18,3	2,69

The results point to a magnifying of the inelastic deformation capacity of beam 2 with regard to beam 1 when it extended concomitantly with the compressive strength and reinforced yield tension.

Another magnifying of this ductility can be observed in beam 3 compared to beam 2 where the compressive strength of the concrete only extended itself.

6 CONCLUSIONS

For the fixed rotation crack model the use of a smaller shear retention factor implicates wider cracks; the variations in β don't modify the maximum values of the crack deformations (ε^{nncr}). For the multi-directional crack model the use of a smaller shear retention factor implicates also wider cracking mainly in the region of pure bending (for β=0,2 eight wider cracks were noticed in this region; for β=0,9 six wider cracks in the same region were noticed); the variations in "β" modify the maximum values of the crack deformations ("β" is inversely proportional to "ε^{nncr}" in this model).

For the rotating crack model the use of a smaller shear retention factor implicates more extended cracking in the region of pure bending; variations in "β"affect the deformation values in the cracks.

The fixed, multi-directional and rotating models predict respectively six, eight and four wider cracks (for β=0,2) in the region of pure bending.

The experimental crack pattern (Figure 9) shows four main cracks in agreement with the rotating smeared crack model.

The results can be observed in the values of the plastic rotation capacity parameters: larger values for the numerical simulation in the DIANA and smaller values for the CASTEM. The results obtained with the FEMOOP were found to be between the ones obtained with the DIANA and the CASTEM (closer to the experimental results).

The results point to a magnification of the inelastic deformation capacity of beam 2 with regard to beam 1 when the compressive strength and steel yield stress are increased.

Another magnification of ductility can be observed in beam 3 compared to beam 2 where the compressive strength of the concrete only is increased.

REFERENCES

Alca, N., Alexander, S.D.B. & MacGregor, J.G. 1997. Effect of size on flexural behavior of high-strength concrete beams, ACI Structural Journal, 94(1), 59-67.

Ashour, S. A. 2000. Effect of Compressive Strength and Tensile Reinforcement Ratio on Flexural Behavior of High Strength Concrete Beams. Elsevier Science Ltd., Engineering Structures, pp. 413 – 423.

Barbosa, M.P. 1998. An Experimental and Numerical Contribution on High Reinforced-concrete Structures: Study of the Anchorage and the Behavior of Bending Beams. Engineering School, São Paulo State University, FEIS, Unesp, 174p.

Comité Euro – International du Béton. 1993. Model Code for Concrete Structures. CEB – FIP MC 90, 437 p.

Corley, G.W. 1966. Rotational capacity of reinforced-concrete beams, ASCE, 92(5), 121-146.

Elwi, A.E. & Hrudey, T.M. 1989. Finite element model for curved embedded reinforcement. Journal of Engineering Mechanics, v.115, n.4, pp.740-754.

Hillerborg, A. 1988. Rotational capacity of reinforced-concrete beams, Norwegian Concrete Research", publication n.7, 121-134.

Homayoun, H.A. & Mitchell, D. 1996. Analysis of bond stress distributions in pullout specimens. Journal of Structural Engineering, v.122, n.3, pp.255-261.

Kani, G.N.J. 1967. How safe are our large reinforced-concrete beams, ACI Journal, 64(3), 128-141.

Kreller, H. 1989. Zum nicht-linearen Trag- und Verformungsverhalten von Stahlbetonstabtragwerken unter Last- und Zwangeinwirkung. Dissertation, Universitat Stuttgart.

Leslie, K.E., Rajagopalan, K.S. & Everard, N.J. 1976. Flexural behavior of high strength concrete beams, ACI Structural Journal, 73(9), 517-521.

Ottosen, N.S. 1977. A failure criterion for concrete. Journal of the Engineering Mechanics Division, v.103, n.4, pp.527-535.

Shin, S.W., Gosh, S.K. & Moreno, J. 1989. Flexural ductility of ultra high strength concrete members, ACI Structural Journal, 86(4), 394-400.

Tognon, G., Ursella, P. & Coppetti, G. 1980. Design and properties of concretes with stregth over 1500kgf/cm2. ACI Structural Journal, 77(3), 171-178.

Walraven, J. & Lehwalter, N. 1994. Size effects in short beams loaded in shear, ACI Structural Journal, 91(5), 585-593.